Journal of Pharmaceutical and Biomedical Analysis 243 (2024) 116081

Contents lists available at ScienceDirect

Journal of Pharmaceutical and Biomedical Analysis

journal homepage: www.journals.elsevier.com/journal-of-pharmaceutical-and-biomedical-analysis

A metabolomics footprinting approach using GC-MS to study inhibitory effects of the fungal metabolite diplopyrone C against nosocomial pathogen biofilms

Maria Michela Salvatore [a,b,*,1], Angela Maione [b,2], Marianna Imparato [b], Francesco Salvatore [b,3], Marco Guida [b,c,4], Emilia Galdiero [b,*,5], Anna Andolfi [a,6]

[a] Department of Chemical Sciences, University of Naples Federico II, Naples 80126, Italy
[b] Department of Biology, University of Naples Federico II, Naples 80126, Italy
[c] BAT Center-Interuniversity Center for Studies on Bioinspired Agro-Environmental Technology, University of Naples Federico II, Portici, NA 80055, Italy

ARTICLE INFO

Keywords:
Mass spectrometry
Candida albicans
Klebsiella pneumoniae
Botryosphaeriaceae
Diplodia corticola
α-Pyrones

ABSTRACT

Seen initially as wonder drugs, the widespread and often inappropriate use of antibiotics led to the development of microbial resistances. As a result, a true emergency has arisen, and a significant need has emerged to discover and develop new safe and valuable antibiotics. The captivating chemical structure of the fungal metabolite diplopyrone C has caught our attention as an excellent candidate for a circumstantial study aimed at revealing its antimicrobial and antibiofilm activities. In this work, we describe the full analytical strategy from the isolation/identification to the evaluation of the metabolomics effect on target microorganisms of this fungal metabolite. Our results show interesting antimicrobial and antibiofilm activities of diplopyrone C against two frequently isolated nosocomial pathogens (i.e., the fungus *Candida albicans* and the gram-negative bacterium *Klebsiella pneumoniae*). Moreover, a GC-MS based metabolomics footprinting approach gave an insight into the uptake and excretion of metabolites from and into the culture medium as a response to the presence of this active substance. The workflow employed in this study is suitable to exploit natural resources for the search of lead compounds for drug development.

1. Introduction

In recent years the scientific community has particularly focused on the development of new antibiotics due to the concerning phenomenon of conventional antimicrobials becoming increasingly ineffective at fighting infectious diseases [1]. The steady increase in the number of registered cases of *Candida* infections annually, which could be most likely related to the development of resistance to antimicrobial drugs, represents an excellent example of the urgent need of novel antimicrobial drugs [2].

Moreover, the capacity of many nosocomial pathogens to form biofilms on different medical devices and surfaces has a profound impact on their capacity to cause human diseases by facilitating their refractoriness to medical therapy [3]. In fact, biofilms are a major cause of persistent infections by clinically important pathogens worldwide. Therefore, nosocomial pathogens are serious threats especially for hospitalized and immunocompromised patients because they can be easily transmitted through person-to-person, environment or contaminated water and food, infected individuals, contaminated healthcare personnel's skin or contact with surfaces [4].

Within the current scenario, characterized by an ever-increasing need for new and beneficial compounds to deal with the emergence of

* Corresponding author at: Department of Chemical Sciences, University of Naples Federico II, Naples 80126, Italy
E-mail addresses: mariamichela.salvatore@unina.it (M.M. Salvatore), egaldier@unina.it (E. Galdiero).
[1] https://orcid.org/0000-0001-8318-3065
[2] https://orcid.org/0000-0002-4981-8837
[3] https://orcid.org/0000-0003-0212-1271
[4] https://orcid.org/0000-0001-6805-0408
[5] https://orcid.org/0000-0001-8116-0839
[6] https://orcid.org/0000-0001-8949-3654

https://doi.org/10.1016/j.jpba.2024.116081
Received 8 November 2023; Received in revised form 28 February 2024; Accepted 29 February 2024
Available online 2 March 2024

potentially lethal infections and multi-resistant microorganisms, the spotlight is on fungal secondary metabolites which are low molecular weight compounds belonging to different classes of natural substances and which, due to their enormous structural diversity, are potentially capable of a broad spectrum of bioactivities and functions. For this reason, fungi represent amazing sources of biologically active metabolites that are used in the production of clinically important drugs [5].

In the last decades, the biosynthetic ability of fungi from the family Botryosphaeriaceae was particularly regarded [6,7]. Among them, *Diplodia* species produce several secondary metabolites with original structures and bioactivities (e.g., diplopyrones, diplodialides, diplobifuranylones, diplofuranones, diploquinones, pinofuranoxins, sphaeropsidins) [8,9]. However, due to their extraordinary capacity for synthesizing bioactive compounds, the list of secondary metabolites from *Diplodia* species is in continuous update which proves the great interest of researchers all over the world on the metabolic potential of this fungal genus. Within this framework, recently, our research group reported the isolation and structural elucidation of the 5,6-dihydropyran-2-one, commonly named diplopyrone C (Fig. 1), from cultures of an isolate of *Diplodia corticola* associated with *Quercus suber* [10].

Due to its newly characterization, diplopyrone C has not yet been investigated for its bioactivities. This compound has a captivating chemical structure composed of an α-pyrone functionalized with a side chain containing an epoxide ring. These structural features make diplopyrone C an excellent candidate of an investigational activity aimed at the discovery of new antibiotics. In fact, α-pyrones are highly recognised as promising compounds due to a huge variety of bioactivities, including antimicrobial [11], antitumor [12], cytotoxic [11]. Moreover, the presence of an epoxide group on the side chain of diplopyrone C could play a significant role in its biological activity because it is known to be highly reactive and, for this reason, responsible of the bioactivities of several natural products [13]. Based on these premises, diplopyrone C is of considerable interest for circumstantial studies aimed at revealing its biological activities.

The experimental design of this study starts with the isolation and identification of diplopyrone C from cultures of *D. corticola*. Subsequently, the antimicrobial and antibiofilm properties of the obtained pure compound have been investigated against two frequently isolated nosocomial pathogens (i.e., the fungus *Candida albicans* and the gram-negative bacterium *Klebsiella pneumoniae*) revealing that biofilms of both tested pathogens are significantly inhibited by diplopyrone C. Our strategy allows to support the favourable results obtained from the antibiofilm assays by metabolomics investigation. To achieve this goal, a GC-MS based metabolomics approach is implemented that provides detailed information on changes in the microbial uptake and excretion of metabolites from and into the culture medium as a response to the active substance.

Accurate and reliable identification of compounds is one of the most important reasons for choosing GC-MS in this metabolomics study.

Overall, in this work we offer a snapshot of the physiological state of *C. albicans* and *K. pneumoniae* in the presence of diplopyrone C and demonstrate a workflow that can be employed to gather valuable information on potential candidates for drug development.

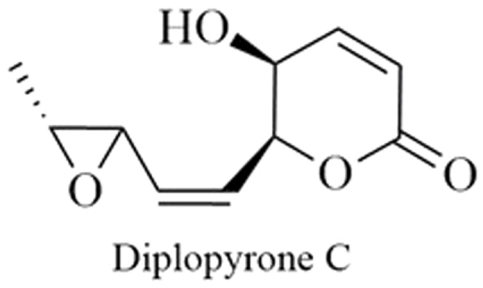

Fig. 1. Chemical structure of 5,6-dihydropyran-2-one (diplopyrone C).

2. Material and methods

2.1. Production and isolation of diplopyrone C

Diplopyrone C used in this study was extracted from an isolated *Diplodia corticola* strain (B305) recovered from *Quercus suber*, producing the novel 5,6-dihydropyran-2-one along with several known metabolites [10]. Liquid cultures of *D. corticola* were prepared as previously reported [10] by inoculating mycelial plugs from actively growing cultures in Czapek-Dox broth (Oxoid, Thermo Scientific, Waltham, MA, USA) amended with 2% cornmeal in 500 mL Erlenmeyer flasks containing 250 mL of the substrate which were kept in darkness on a stationary phase at 25 °C for 30 days. The culture broth and mycelia were homogenized in a mixer with a mixture of H_2O:MeOH (45:55 *v/v*, 1% NaCl) and subsequently centrifuged at 5000 × *g* and 10 °C. This procedure was repeated twice, supernatants were collected and MeOH was evaporated under reduced pressure to obtain an aqueous solution for the subsequent extraction (3 times) with ethyl acetate at native pH (= 6.0). The organic phases were combined, dried with anhydrous Na_2SO_4, and evaporated under reduced pressure, yielding crude extract as brown oil. The crude extract was submitted to fractionation by column chromatography and thin-layer chromatography on silica gel, eluted with diverse polarity solvents. Diplopyrone C (yellowing amorphous solid) was identified by comparing NMR data with previously reported data (Fig. S1 and Fig. S2) [10]. ^{1}H NMR and ^{13}C spectra were recorded on a Bruker AMX instrument (Bremen, Germany) at 100 and 400 MHz in $CDCl_3$. The same solvent was used as internal standard. HRESI-TOF mass spectrum was measured on an Agilent Technologies ESI-TOF 6230DA instrument in the positive ion mode (Milan, Italy) (Fig. S3).

A stock solution of accurately known concentration of diplopyrone C, prepared by dissolving a weighted amount of the pure compound in 5% dimethyl sulfoxide (DMSO), served as the source of diplopyrone C for biological assays described below.

2.2. Microbial strains and cultural conditions

Candida albicans ATCC 90028 and *Klebsiella pneumoniae* ATCC 13883 were used in this study. The two strains were stored in 15% (*v/v*) glycerol stocks at −80 °C. For the experiments, cells were cultured at 37 °C for 24 h into Tryptic Soy Broth (TSB, Oxoid, Basingstoke, UK) supplemented (*C. albicans*) or not (*K. pneumoniae*) with 1% *w/v* glucose (VWR Chemicals, Radnor, Pennsylvania, United States of America). Then, the cells were washed twice using sterile phosphate-buffered saline (PBS, Oxoid Ltd., Basingstoke, UK), and standardized to 1 × 10^6 cells mL^{-1} in the respective culture medium.

2.3. Cell cultures

PNT1A cells ECACC 95012614 (Human prostate cell line established by immortalization of adult prostateepithelial cells) were used in this study. Cells were propagated in RPMI 1640 medium (Thermo Fisher Scientific, Waltham, MA, USA) supplemented with 10% of Fetal Bovine Serum (FBS, Sigma-Aldrich, St. Louis, MO, USA), 2 mM L-glutamine (Sigma Aldrich, St. Louis, MO, USA) and 100 U/mL penicillin/streptomycin (Sigma Aldrich, St. Louis, MO, USA) incubated at 37 °C with 5% CO_2. When the cells reached 70% of confluence, they were detached enzymatically with 0.25% Trypsin/EDTA solution (Sigma Aldrich, St. Louis, MO, USA) and cultured into new flasks for following experiments.

2.4. Minimum inhibitory concentration and MBC/MFC

The minimum concentration of diplopyrone C able to inhibit by 90% the microbial growth was evaluated following the Clinical and Laboratory Standards Institute (CLSI M27-A3 and M07-A9) microdilution

reference method with some modifications [14]. Diplopyrone C at concentration ranging from 0.001 to 5.0 g L^{-1} was added into each well of a 96-well microplate containing 100 μL of 1 × 10^6 cells mL^{-1} microbial suspension. The plate was incubated at 37 °C for 24 h and microbial growth was determined at 590 nm wavelength with a microplate reader (Synergy H4; Bio-Tek Instruments, Agilent Technologies, Winooski VT05404 USA). The Minimum Fungicidal Concentration (MFC) and the Minimum Bactericidal Concentration (MBC) were established plating 100 μL of each well with no visible microbial growth onto Tryptic Soy Agar (TSA, Oxoid, Basingstoke, UK) and incubated at 37 °C for 24/48 h. The MFC and MBC were defined as the lower concentration that inhibited growth on the agar plates. The ratio between MFC or MBC and MIC were calculated to determine whether the substance had fungistatic/bacteriostatic (MBC/MIC or MFC/MIC ≥ 4) or fungicidal/bactericidal (MBC/MIC or MFC/MIC < 4) activity [15].

2.5. Biofilm inhibition and eradication

The ability of diplopyrone C to prevent biofilm formation and eradicate mature biofilms, was investigated as reported previously [16].

Inhibition of biofilm formation was assessed, in 96-well microplates, adding 100 μL of 1 × 10^6 cells mL^{-1} microbial suspension in TSB (with 1% glucose *w/v* for *C. albicans*) and 100 μL of a suitably diluted diplopyrone C solution to span concentrations from 0.025 to 1.0 g L^{-1}. The plates were incubated at 37 °C for 24 h.

Eradication was performed by adding to the mature biofilms, previously formed in 96-well microplates for 24 h, diplopyrone C at concentrations ranging from 0.125 to 1 g L^{-1} and incubated at 37 °C for other 24 h.

Total biofilm biomass was detected by the crystal violet (CV) assay [17] with some modifications. Plates were washed three times with PBS to remove the non-adhered cells. After biofilms were fixed at 37 °C for 1 h, 200 μL of CV was added to each well for 15 minutes. The excess was washed with PBS, and biofilms were resuspended by adding 300 μL of acetic acid at 33% (*v/v*).

Absorbance at 570 nm was read using a microplate reader (Synergy H4; Bio-Tek Instruments, Agilent Technologies, Winooski VT05404 USA). The percentage of inhibition and eradication was calculated as [(OD570 of the control − OD570 of the treated)/OD570 of the control] × 100. Each experiment was conducted in triplicate.

2.6. Cytotoxicity assay

PNT1A cells were used to assess the cytotoxicity of diplopyrone C, according to our previous protocol [18]. Cells at concentration of 5 × 10^3 cells per well in 100 μL of growth medium were added in 96-well microplates and incubated at 37 °C at 5% CO_2 for 24 h. After that, different concentrations of diplopyrone C (from 0.00312 to 2.0 g L^{-1}) were inserted into each well and the plates were incubated at 37 °C at 5% CO_2 for 24 h. Untreated cells served as control. The cell viability was determined by colorimetric method using MTT assay (3-[4,5-dimethylthiazol-2-yl]-3,5 diphenyl tetrazolium bromide) according to manufacturer's instruction. The absorbance at 570 nm was read in a microplate reader (Synergy H4; Bio-Tek Instruments, Agilent Technologies, Winooski VT05404 USA). The percentage of cell viability was calculated as (OD570 of the control / OD570 of the treated) × 100.

2.7. Metabolomics analysis

2.7.1. Sample preparation

For the investigation of changes induced by diplopyrone C on *C. albicans* and *K. pneumoniae* metabolism, biofilm cultures of the two microorganisms in 96-well microtiter plates were incubated for 24 h at 37 °C. Following incubation, the liquid medium (100 μL) was carefully collected from the wells of the microplate, transferred into Eppendorf tubes, and centrifuged (5000 × *g*, 10 min). Then, supernatants were dried under a stream of nitrogen, and the residues were derivatized (trimethylsilylated) with *N,O*-bis(trimethylsilyl)-trifluoroacetamide (BSTFA) (Fluka, Buchs, Switzerland), as previously described [19]. During the derivatization process, 0.125 g L^{-1} of benzocaine was added to each sample as an internal standard. For each condition, three samples were extracted from three replicated cultures and GC-MS analysis of each sample was replicated three times.

2.7.2. GC-MS analysis

Trimethylsilyl derivatives were analyzed using an Agilent 6850 GC instrument (Milan, Italy) coupled to an Agilent 5973 Inert MS. 2 μL of each sample were injected in splitless mode into an HP-5MS capillary column ((5%-phenyl)-methylpolysiloxane stationary phase). The injector temperature was 250 °C, and the temperature ramp raised the column temperature from 70 °C to 280 °C according to the following temperature program: 70 °C for 1 min; 10 °C · min^{-1} until the column temperature reached 170 °C; 30 °C·min^{-1} until the column temperature reached 280 °C; 280 °C for 5 min. Helium was used as a carrier gas at a flow rate of 1 mL · min^{-1}. The solvent delay was set to 4 min. Measurements were performed under electron impact (EI) ionization (70 eV) in full scan mode (*m/z* 29–550) at a frequency of 3.9 Hz. The EI ion source and quadrupole mass filter temperatures were kept, respectively, at 200 and 250 °C.

2.7.3. Data processing and statistical analysis

GC-MS data were deconvoluted using the National Institute of Standards and Technology (NIST) program Automated Mass Spectral Deconvolution and Identification System (AMDIS) [20,21], and then "conserved" components across the full set of 54 observations (3 technical replicates for each of 18 samples from 9 cultures of *C. albicans* and 9 cultures of *K. pneumoniae*) were tracked and listed using SpectConnect program. The 54 observations span 6 cultural conditions or classes each collecting 9 observations. Class 1Ca-Control comprises observations on untreated biofilm cultures of *C. albicans*; classes 2Ca-Treatment125 and 3Ca-Treatment250 collect observations from *C. albicans* cultures treated with 0.125 g L^{-1} and 0.250 g L^{-1}, respectively, of diplopyrone C. Analogously, class 4Kp-Control collects observations from untreated *K. pneumoniae* cultures while the culture medium for observations in the 5Kp-Treatment025, 6Kp-Treatment050 classes was fortified with 0.025 g L^{-1} and 0.050 g L^{-1} of diplopyrone C, respectively.

Technically, in the context of SpectConnect software, a conserved component is one that consistently persists in replicate samples (at least in 75% of the observations in one condition or class). The SpectConnect program creates a matrix (Integrated Signal matrix, IS matrix) with rows corresponding to conserved components and columns corresponding to observations. An element of the IS matrix is a value which corresponds to the integrated signal, or abundance, attributed to the component in the deconvoluted Total Ion Current Chromatogram (TICC) acquired in the observation identified by the column label.

Data in the IS matrix created by the SpectConnect program were analysed with our in-house program developed in MATLAB R2023a (Mathworks, Natick, MA, USA) [22].

First, the abundances in each column of the IS matrix were normalized with respect to the corresponding signal of the internal standard added during the preparation of the samples (i.e., 0.125 g L^{-1} benzocaine). Then, components identification was performed by matching their deconvoluted EI mass spectra at 70 eV with those stored in the NIST 20 mass spectral library [23] and the Golm metabolome database [23,24]. The identification was further supported by Kovats retention index (RI) calculated for each component by the Kovats equation using chromatographic data from a standard *n*-alkane mixture in the range C7–C40 (Sigma-Aldrich, Saint Louis, MO, USA) analysed under the same conditions. After the time-consuming identification process, the original IS matrix was reduced to a 52×54 IS matrix by deleting rows corresponding to non-identified components (i.e., we were able to identify 52 metabolites out of 223 components listed in the IS

matrix). Because data pertaining to *C. albicans* and *K. pneumoniae* cultures need to be analysed separately, the 52×54 IS matrix was split into a 50×27 IS matrix describing metabolite levels in *C. albicans* cultures and a 40×27 IS matrix describing metabolite levels in *K. pneumoniae* cultures. These two IS matrices are employed for all successive evaluations of the effects of diplopyrone C on *C. albicans* and *K. pneumoniae* metabolism, respectively.

For unsupervised multivariate statistical analyses, i.e., Hierarchical Clustering Analysis (HCA), the IS matrix associated to each microorganism was standardized so that each row had mean zero and standard deviation 1 (Z-Score standardization).

Supervised univariate analysis of data in the IS matrix was performed in order to compare metabolites levels, one by one, in a selected pair of classes. This allows the determination of metabolites which levels in the extracellular medium are significantly different between two selected conditions (classes). Within this framework, for each identified metabolite, two arrays of nine IS values (one array for each of the two compared conditions) are extracted from the IS matrix and passed to the MATLAB's "ttest2" function. This function compares the averages of the two vectors using unpaired Student's *t*-test and returns, among other statistics, a *p*-value. After this, for each metabolite, a fold change (FC) value is calculated as the ratio of the averages of the two compared vectors. A metabolite is considered to be differentially expressed between two compared classes if the associated *p*-value is lower than 0.05 (i.e., the significance threshold is set to 5%) and the associated fold change is greater than 2 (upregulated) or lower than 0.5 (downregulated).

3. Results

3.1. Production of Diplopyrone C

Diplopyrone C was purified from cultures of *D. corticola* strain (B305) isolated from *Q. suber*, using chromatographic processes (see Material and Methods). It was identified comparing the mass spectrometry and NMR spectroscopic data with a previous report (see Figs S1-S3) [10].

3.2. Antimicrobial, antibiofilm and cytotoxic activities

Diplopyrone C showed promising results in the preliminary antibacterial/antifungal screening against the pathogens *C. albicans* ATCC 90028 and *K. pneumoniae* ATCC 13883.

As showed in Table 1, the MIC90 (i.e., the lowest concentration of tested product required to inhibit bacterial/fungal growth by 90%) of diplopyrone C was 2.0 g L^{-1} for *C. albicans* and 0.5 g L^{-1} for *K. pneumoniae*, respectively.

Subsequently, we also evaluated the MFC (Minimum Fungicidal Concentration) and MBC (Minimum Bactericidal Concentration) of diplopyrone C which, respectively, represent the lowest product concentration that prevents growth of the fungus or bacterium on agar plates incubated at 37 °C for 24/48 h. The ratio MFC/MIC was calculated to evaluate whether diplopyrone C has fungistatic (MFC/MIC ≥ 4) or fungicidal (MFC/MIC < 4) activity against *C. albicans*. Analogously, we calculated the ratio MBC/MIC to evaluate the bacteriostatic/bactericidal activity of diplopyrone C against *K. pneumoniae*. As shown in Table 1, because both MFC/MIC and MBC/MIC ratios are below 4, it is concluded that diplopyrone C exerts fungicidal/bactericidal activity against the tested microorganisms.

Table 1
MIC, MFC or MBC of diplopyrone C against *C. albicans* ATCC 90028 and *K. pneumoniae* ATCC 13883. The ratio MFC/MIC or MBC/MIC < 4 indicated fungicidal or bactericidal effect.

	MIC (g L^{-1})	MBC or MFC (g L^{-1})	MBC/MIC or MFC/MIC ratio	
C. albicans ATCC 90028	2.0	5.0	2.5	fungicidal
K. pneumoniae ATCC 13883	0.5	0.5	1.0	bactericidal

Biofilms formation by *C. albicans* and *K. pneumoniae* was challenged by growing biofilms cultures in 96-well microplates for 24 h at 37 °C in presence of increasing concentrations of diplopyrone C ranging from 0.025 to 1 g L^{-1}. Measures of biofilm biomass were carried out with crystal violet (CV) colorimetric method (see Material and Methods).

From Fig. 2A, we see that, at the two highest concentration tested (0.5 and 1 g L^{-1}), diplopyrone C induced biofilm inhibition of about 70% and 80% for *C. albicans*. For *K. pneumoniae*, an inhibition of 100% is observed at such high concentrations (i.e., 0.5 and 1 g L^{-1}) as one might anticipate from the fact that they correspond respectively to the bacterial MIC and double the MIC. Nevertheless, inhibition of biofilm formation by *K. pneumoniae* persists at sub-MIC concentrations according to the pattern shown in Fig. 2A by light gray bars.

Results of the degradative effect of diplopyrone C (at concentrations ranging from 0.125 to 1 g L^{-1}) on mature biofilms of the two tested microorganisms follow the patterns described in Fig. 2B. For instance, we see that *C. albicans* and *K. pneumoniae* biofilms, previously grown for 24 h at 37 °C in 96-well microtiter plate, were eradicated at a rate of ~40% and of ~50%, respectively, by incubating for 24 h at 37 °C in presence of 1 g L^{-1} of diplopyrone C.

The cytotoxic activity of diplopyrone C was evaluated on human prostate cell line (PNT1A) using the colorimetric MTT assay. Cells were exposed, in 96-well microplates for 24 hours at 37 °C, to diplopyrone C concentrations ranging from 0.00312 g L^{-1} to 2 g L^{-1}. The results expressed as the average percentage of cell viability relative to the viability of untreated cells (control) are displayed in Fig. 3. At the highest concentrations (0.5, 1 and 2 g L^{-1}), diplopyrone C exhibited a cytotoxic effect on the cells since a mortality rate of ~40%, ~50% and ~70%, respectively, was recorded. However, at lower concentrations, no significant cell damage was detected.

3.3. Metabolomics analysis

3.3.1. Data pre-processing and general results

To evaluate the effects of the fungal compound diplopyrone C on metabolic profiles of *C. albicans* and *K. pneumoniae*, biofilm cultures of *C. albicans* and *K. pneumoniae* were grown for 24 h at 37 °C in presence and absence of this compound in 96-well microtiter plates. According to the results of biological assays reported in the previous section, the culture medium was enriched with two sub-MIC concentrations of diplopyrone C (i.e., 0.125 and 0.250 g L^{-1} for *C. albicans* and 0.025 and 0.050 g L^{-1} for *K. pneumoniae*). The changes in the metabolic profile eventually induced by diplopyrone C were tracked by using a GC-MS-based metabolomics footprinting strategy. Altogether, we have acquired 54 observations (GC-MS chromatograms) which span six different cultural conditions (or classes) corresponding to treated and untreated *C. albicans* biofilm cultures (i.e., 1Ca-Control, 2Ca-Treatment125, 3Ca-Treatment250) and *K. pneumoniae* biofilm cultures (i.e., 4Kp-Control, 5Kp-Treatment025, 6Kp-Treatment050). Clearly, the three last digits in labels identifying different classes allude to the diplopyrone C concentration in the corresponding culture medium.

Each class comprised nine observations, corresponding to three technical for each of three biological replicates, acquired under identical acquisition and cultural conditions.

As reported in Material and Methods, the GC–MS datafiles were processed with AMDIS and SpectConnect programs to create a matrix (Integrated Signal matrix, IS matrix), with rows corresponding to "conserved metabolites" and columns corresponding to observations, and which will be the basis of the following evaluations. Each cell of the IS matrix contains the abundance (i.e., the integrated signal in the deconvoluted TIC chromatogram) of the component identified by the row label in the observation identified by the column label. A constant

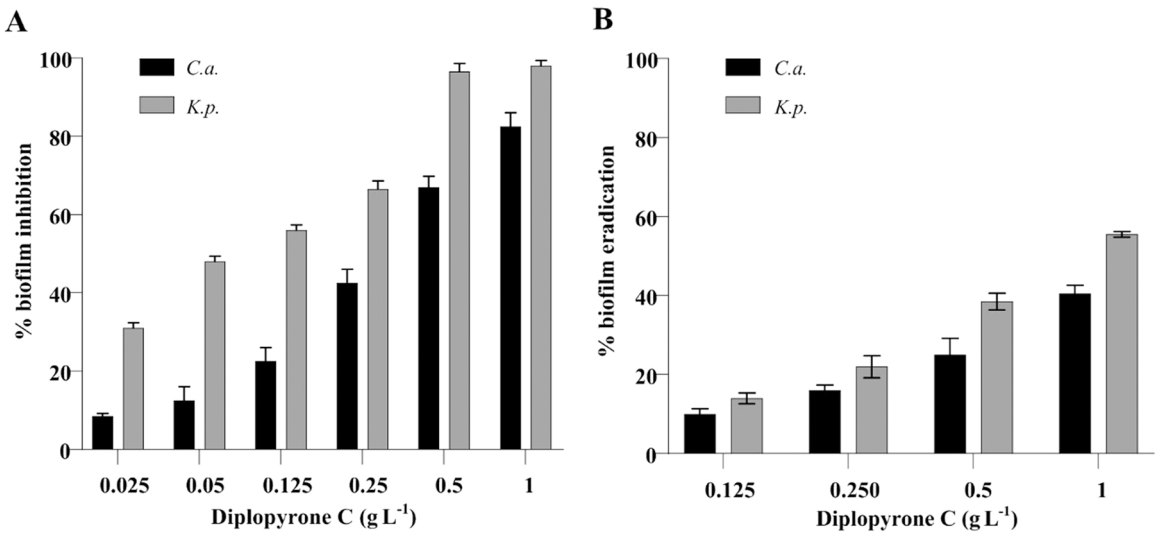

Fig. 2. Effect of diplopyrone C on the biofilms of *C. albicans* and *K. pneumoniae*. Inhibition (A) and eradication (B). For inhibition assays biofilms were quantified after 24 h growth at 37 °C. For eradication assays, biofilms, previously grown at 37 °C for 24 h in microplates wells, were quantified after 24 h exposure to diplopyrone C at 37 °C. Biofilm biomass was quantified with the colorimetric CV method. Results are shown as the mean of inhibition and eradication percentage of three indipendend experiments ± standard deviation.

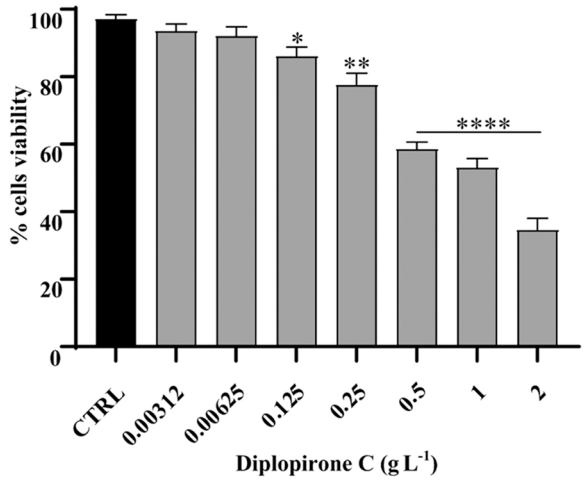

Fig. 3. Cytotoxic effects on human prostatic cell line PNT1A induced by 24 h exposure to diplopyrone C at different concentrations. ** *p*-value < 0.01, *** *p*-value < 0.001, **** *p*-value < 0.0001 (Tukey's test). The results are expressed as the average percentage of cell viability relative to the viability of untreated cells (control) ± standard deviation evaluated from three independent tests.

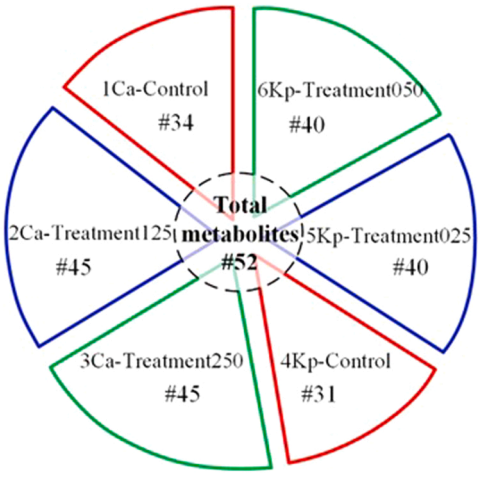

Fig. 4. Distribution among classes (i.e., 1Ca-Control, 2Ca-Treatment125, 3Ca-Treatment250, 4Kp-Control, 5Kp-Treatment025, 6Kp-Treatment050) of identified metabolites in biofilm cultures of *C. albicans* and *K. pneumoniae* in presence and absence of diplopyrone C.

concentration of benzocaine was added as an internal standard to each sample before analytical processing and abundances in each column of the IS matrix were normalized with respect to the corresponding benzocaine signal to compensate for random and instrumental factors which can affect measured signals from sample to sample.

The dataset comprised 223 chromatographic peaks (components), and, among them, we identified 52 metabolites by comparing the deconvoluted 70 eV EI mass spectrum of each component with mass spectra of known compounds in commercially available MS libraries and by their Kovats retention index.

The identified metabolites are distributed among the six classes considered as shown in Fig. 4 and are listed according to their chromatographic retention time (RT) and Kovats retention index (RI) in Table 2.

The last column in Table 2 contains a 1 × 6 ordered array of digits (from 1 to 6) defining the coordinates of each identified compound in the space of classes. The coordinates associated to each metabolite indicate its presence/absence in each of the examined cultural conditions. For instance, the reported coordinates (i.e., {0,2,3,0,5,6}) for the metabolite (23)-cyclo(alanyl-glycyl) indicate that this metabolite has been detected only in classes 2Ca-Treatment125, 3Ca-Treatment250, 5Kb-Treatment025 and 6Kp-Treatment050 while it is absent in the untreated control samples of both *C. albicans* and *K. pneumoniae*. The exploration of the data in Table 2 reveals that identified metabolites belongs to primary and secondary metabolic pathways, including amino acids, vitamins, sugars and sugar alcohols.

To establish the metabolic effects induced by diplopyrone C on each of the two targeted microorganisms, the IS matrix was split into two IS sub-matrices containing respectively only the data pertaining to the *C. albicans* and *K. pneumoniae* cultures. As can be deduced from the coordinates in Table 2, the two IS sub-matrices had different sizes. In fact, the IS matrix associated to *C. albicans* exposed 48 rows (metabolites) while the IS matrix associated to *K. pneumoniae* exposed 40 rows.

Table 2
Identified metabolites from GC-MS metabolomic analysis of *C. albicans* and *K. pneumoniae* cultures in presence and absence of diplopyrone C. RT represents retention time, RI represents Kovats retention index and TMS is the trimethylsilyl function, $(CH_3)_3Si$-. The ordered array of digits in the column labelled "Coordinates" indicates ordinately the class membership of metabolites (1Ca-Control = 1; 2Ca-Treatment125 = 2; 3Ca-Treatment250 = 3, 4Kp-Control = 4; 5Kp-Treatment025 = 5; 6Kp-Treatment050 = 6). To facilitate exploration of results, a numeric label has been incorporated to the name of each metabolite.

Common Name	RT (min)	RI	Coordinates
(1)-Propylene glycol (i.e. 1,2-propanediol), 2TMS	4.239	1028	{0,0,3,0,0,0}
(2)-2,3-Butanediol, 2TMS	4.7715	1068	{0,0,0,4,5,6}
(3)-Diethylcarbamate, TMS	4.9514	1082	{1,0,0,0,0,0}
(4)-Lactic Acid, 2TMS	5.0138	1086	{1,2,3,4,5,6}
(5)-Glycolic acid, 2TMS	5.1631	1098	{0,2,3,4,5,6}
(6)-Pyruvic acid, 2TMS	5.2849	1107	{1,2,3,4,5,6}
(7)-Alanine, 2TMS	5.4678	1121	{1,2,3,4,5,6}
(8)-Glycine, 2TMS	5.7026	1139	{1,2,3,4,5,6}
(9)-Hydracrylic acid, 2TMS	5.9732	1159	{1,2,3,4,5,6}
(10)-Valine, 2TMS	6.9301	1231	{1,2,3,4,5,6}
(11)-Leucine, 2TMS	7.643	1284	{0,2,3,4,5,6}
(12)-Phosphate, 3TMS	7.7065	1289	{1,2,3,4,5,6}
(13)-Glycerol, 3TMS	7.7542	1292	{1,2,3,0,0,0}
(14)-Niacin, TMS	7.9448	1307	{0,2,3,0,5,6}
(15)-Isoleucine, 2TMS	7.976	1309	{1,2,3,4,5,6}
(16)-Proline, 2TMS	8.02	1313	{1,2,3,4,5,6}
(17)-Succinic acid, 2TMS	8.1454	1322	{1,2,3,4,5,6}
(18)-2,3-Dihydroxy-2-methylpropanoic acid, 3TMS	8.3158	1335	{1,2,3,4,5,6}
(19)-Glyceric acid, 3TMS	8.4364	1345	{1,2,3,4,5,6}
(20)-Uracil, 2TMS	8.5087	1350	{1,2,3,0,5,6}
(21)-2,5-Dimethyl-4-pyrimidinamine, TMS	8.5319	1352	{0,2,3,4,5,6}
(22)-Serine, 3TMS	8.8258	1375	{1,2,3,0,5,6}
(23)-Cyclo(alanyl-glycyl), 2TMS	9.0818	1394	{0,2,3,0,5,6}
(24)-Threonine, 3TMS	9.1616	1400	{1,2,3,4,5,6}
(25)-3-Hydroxy-2,3-dihydromaltol, 2-O-TMS	9.9153	1462	{0,0,0,4,5,6}
(26)-2-Aminomalonic acid, N,O,O,-TMS	10.1882	1484	{1,2,3,0,0,0}
(27)-Malic acid, 3TMS	10.3922	1501	{1,2,3,0,0,0}
(28)-Aspartic acid, 3TMS	10.7188	1538	{1,2,3,4,5,6}
(29)-Oxoproline, 2TMS	10.7457	1541	{1,2,3,4,5,6}
(30)-3,5-bis(trimethylsilyloxy)-3-methylvalerate, TMS	11.0358	1573	{0,0,0,4,5,6}
(31)-3-Aminopiperidine-2,6-dione, 2TMS	11.4381	1623	{0,2,3,0,5,6}
(32)-Glutamic acid, 3TMS	11.5141	1635	{1,2,3,4,5,6}
(33)-Phenylalanine, 2TMS	11.5852	1645	{1,2,3,4,5,6}
(34)-Tartaric acid	11.6987	1662	{0,2,3,4,5,6}
(35)-Asparagine, 3TMS	11.8646	1686	{0,2,3,0,5,6}
(36)-Xylose, 4TMS	11.9857	1705	{0,2,0,0,0,0}
(37)-Arabitol, 5TMS	12.2305	1750	{1,2,3,0,0,0}
(38)-GlyceroPhosphoric acid, 4TMS	12.4392	1788	{1,2,3,4,5,6}
(39)-Benzocaine, TMS (Internal Standard)	12.4716	1794	{1,2,3,4,5,6}
(40)-Terephthalic acid, 2TMS	12.5116	1802	{1,0,0,0,0,0}
(41)-Adenine, 2TMS derivative	12.9092	1887	{0,0,0,0,5,6}
(42)-Tyrosine, 2TMS	12.9786	1902	{1,2,3,4,5,6}
(43)-Pyridoxine, 3TMS	13.0598	1923	{1,2,3,4,5,6}
(44)-Lysine, 4TMS	13.125	1939	{0,2,3,0,5,6}
(45)-Pantothenic acid,3TMS	13.4222	2015	{1,2,3,4,5,6}
(46)-Palmitic Acid, TMS	13.5273	2043	{1,2,3,4,5,6}
(47)-Butyl mannoside, 4TMS	13.6967	2090	{1,2,3,0,0,0}
(48)-Myo-Inositol, 6TMS	13.828	2127	{0,2,3,4,5,6}
(49)-Tryptophan, N.,N.-diacetyl, N1,O-2TMS	14.0756	2199	{0,2,3,4,5,6}
(50)-.alpha.-D-glucopyranose, 1-O-(3-O-(2-methylbutanoyl)-.alpha.-D-glucopyranosyl), 7TMS	16.1929	2659	{1,2,3,0,0,0}
(51)-2-.alpha.-Mannobiose, 8TMS	16.339	2682	{0,2,3,0,5,6}
(52)-Turanose, 8TMS	17.1254	2788	{1,2,3,0,0,0}
(53)-Trehalose 8TMS	17.3441	2814	{1,2,3,0,0,0}

In the following subsections, unsupervised and supervised statistical analyses of the collected GC-MS data are conducted separately for each tested microorganism on the basis of its associated IS matrix. For this we have employed an in-house program developed in the MATLAB environment.

3.3.2. *Metabolomics analysis of C. albicans biofilm cultures in presence and absence of diplopyrone C*

For unsupervised statistical analysis, the IS matrix describing metabolite levels in *C. albicans* cultures was standardized such that rows of the matrix are centered to have mean 0 and scaled to have standard deviation 1. This type of data standardization is known as Z-Score standardization. Standardization is a necessary step to make metabolites equally important regardless of their concentrations in samples.

After standardization, the IS matrix was presented to the MATLAB's "clustergram" function which produced Fig. 5 which summarizes and displays Hierarchical Clustering Analysis (HCA) results for the 27 observations in the IS matrix in the form of a dendrogram and a heatmap of the z-scored clustered IS matrix. Results presented in Fig. 5 are further extended in Figs S4 and S5.

From the dendrogram in Fig. 5 and Fig. S4 there can be no doubt that observations in the IS matrix form only two clusters even though they have been collected under three nominally different treatments. These two clusters are connected by a very high and inconsistent link which implies that observations in the two clusters are quite different from each other. In fact, the cophenetic distance between the two clusters is about 16.7 (see Fig. S4) and the inconsistency coefficient of the link connecting Cluster 1 to Cluster 2 is 1.96.

Inspection of Fig. 5 and Fig. S4 readily shows that the first cluster only contains observations in the class 1Ca-Control while in the second cluster are randomly collected observations in the 2Ca-Treatment125 and 3Ca-Treatment250 classes which appear to be quite similar to each other since they are connected by much less inconsistent links. Thus, the levels of metabolites in cultures of *C. albicans* treated with diplopyrone C are very similar regardless of its concentration in the culture medium (i.e., 0.125 g L^{-1} or 0.250 g L^{-1}).

The reasons for the differences between the above two observations clusters are quite apparent from the heatmap in Fig. 5. Simply, almost all metabolites are present at lower levels in observations in the first cluster (corresponding to the nearly uniformly green slice of the heatmap) compared to observations in the second cluster (corresponding to the nearly uniformly red slice of the heatmap).

We can be confident that the above results are statistically significant and that the hierarchical tree shown in Fig. 5 and Fig. S4 describes accurately the distance between original observations in the IS matrix because the hierarchical tree has a very high cophenetic correlation coefficient (0.93 out of a maximum of 1). A further proof of the statistical validity of our clustering results is produced by the Silhouette Plot in Fig. S5 from which we can see that all observations have a high silhouette value. The silhouette values range from –1 to 1. A high silhouette value indicates that an observation is well matched to its own cluster, and poorly matched to other clusters [25].

In addition to the above clustering analysis, normalized data in the IS matrix associated to *C. albicans* were subjected to supervised univariate analyses in order to reveal further insights into the metabolic differences among the three cultural conditions investigated. To this end, for each metabolite, three 9×1 vectors are extracted from each row of the IS matrix. Each vector contains the 9 integrated signals collected by analysing 3 times each of 3 biological replicated samples in a class. By averaging the integrated signals in each of the three vectors, we readily obtain three values which represent, respectively, the average level of a given metabolite in the three classes 1Ca-Control, 2Ca-Treatment125 and 3Ca-Treatment250. In Fig. 6A the average abundances of all identified metabolites in class 1Ca-Control are compared with corresponding averages in class 2Ca-Treatment125. Analogously, in Fig. 6B, the averages abundances of metabolites in class 2Ca-Treatment125 are compared to the corresponding averages in class 3Ca-Treatment250.

Fig. 6A and B are in perfect agreement with results of HCA analysis. In fact, in Fig. 6A the levels of metabolites in the 2Ca-Treatment125 class are clearly higher than the corresponding levels in class 1Ca-Control

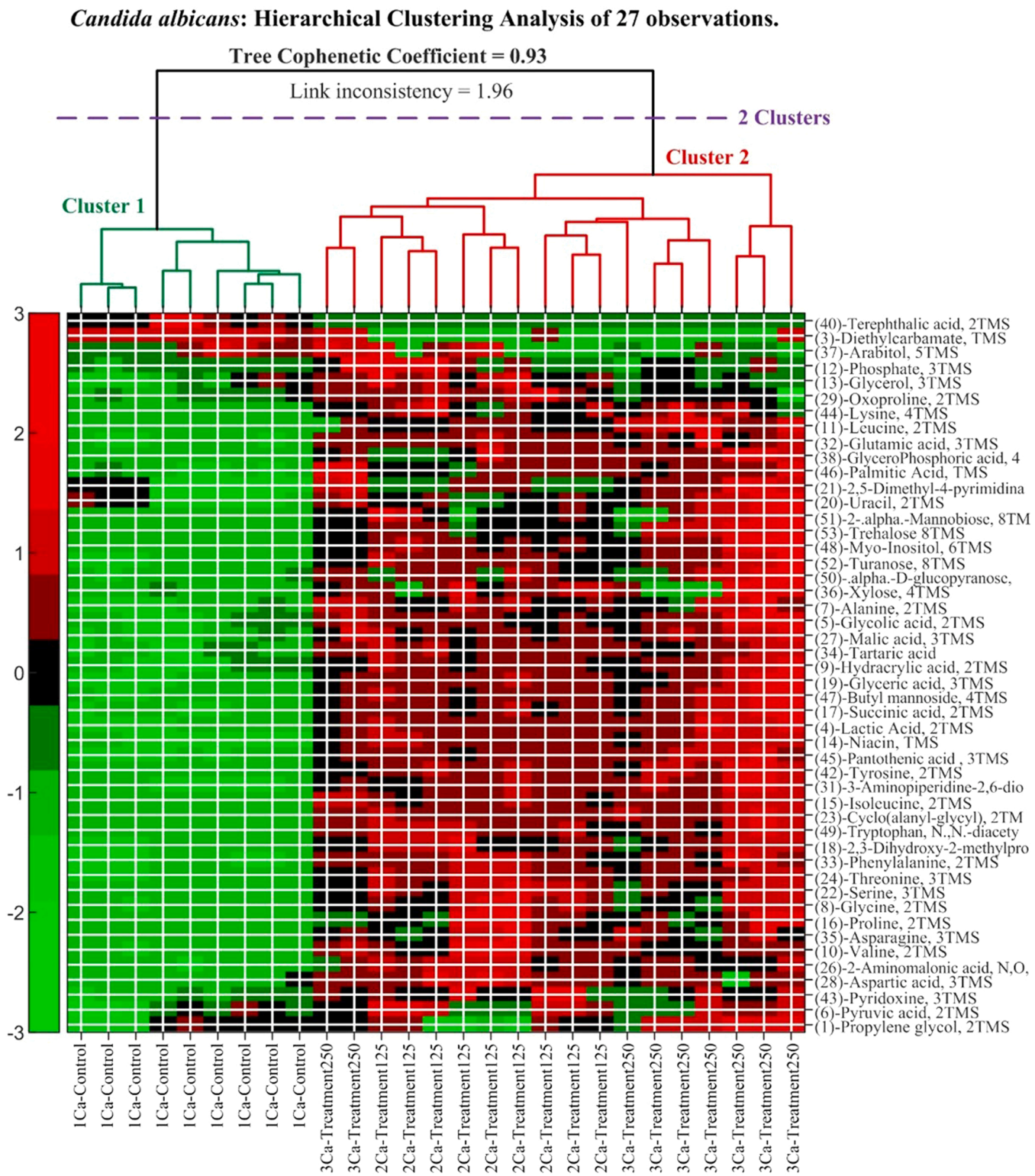

Fig. 5. Clustergram describing Hierarchical Clustering Analysis (HCA) results obtained from metabolomic profiles of biofilm cultures of *C. albicans* grown in presence (i.e., 2Ca-Treatment125, 3Ca-Treatment250) and absence (i.e., 1Ca-Control) of diplopyrone C. Each feature is plotted in red–green colour scale. Since rows of the heatmap are standardized to have zero mean and standard deviation 1 (Z-Score standardization), the red colour (positive) of the tile indicates that the metabolite z-score is above the mean and the green colour (negative) indicates that the metabolite z-score is below the mean; obviously, by definition, the mean z-score is zero and corresponds to black colour in the heatmap. Hierarchical Clustering Analysis was performed by setting the distance metric to "Euclidean" and the linkage parameter to "Complete". Metabolites are identified by using only the first 30 chars of their full name and can be tracked back to the corresponding entry in Table 2 through the associated numeric labels.

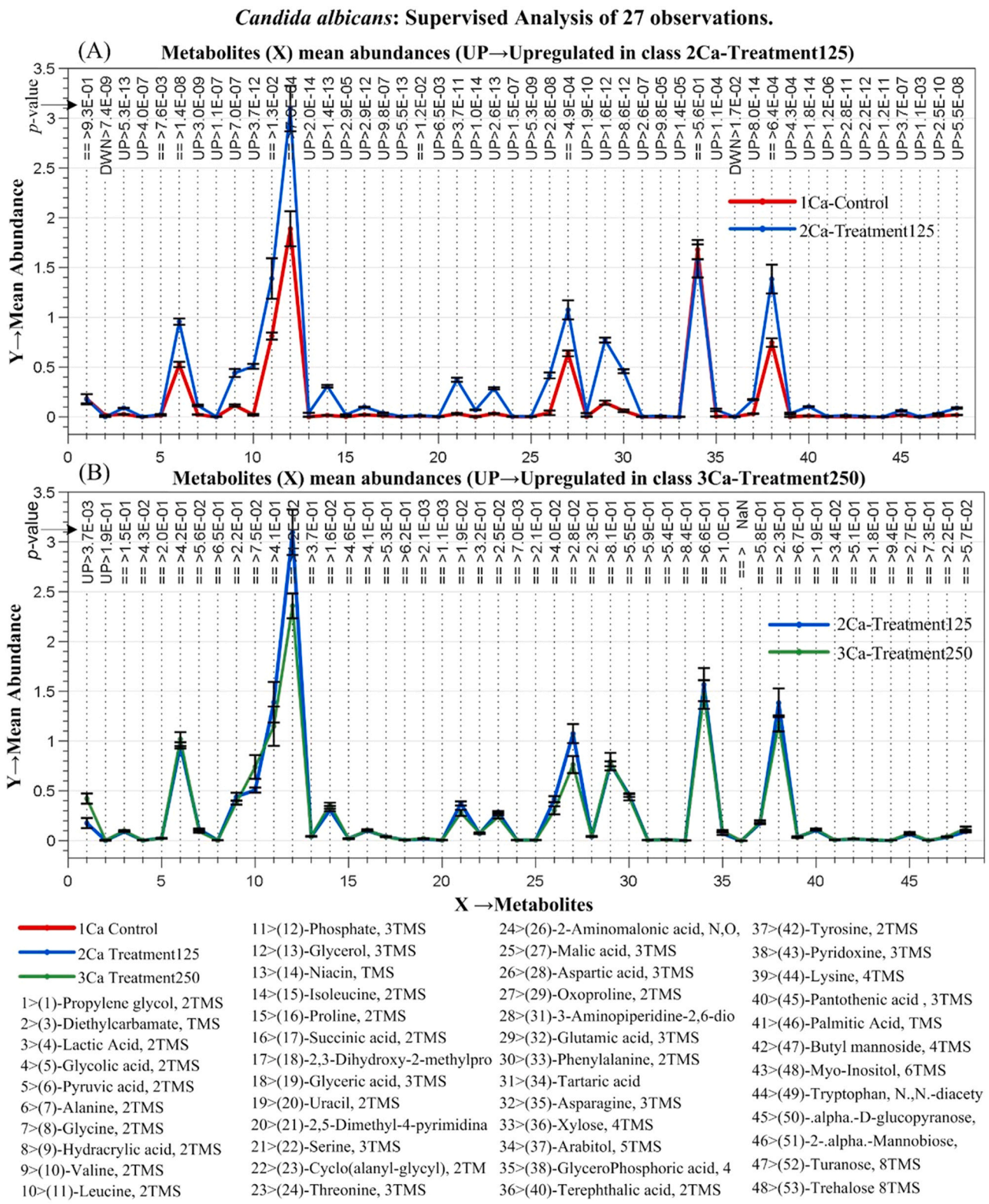

Fig. 6. Results of univariate comparison of biofilm cultures of *C. albicans* in presence (i.e., 0.125 and 0.250 g L^{-1}) and absence of diplopyrone C. (A) 2Ca-Treatment125 vs. 1Ca-Control; (B) 3Ca-Treatment250 vs. 2Ca-Treatment125. For each metabolite, fold change (FC) is defined as the ratio between means of normalized abundances in the two compared classes. Only metabolites with p-value < 0.05 and fold changes greater than 2 or lower than 0.5 are considered to be differentially expressed in the two compared classes as indicated by labels UP (Upregulated) and DOWN (Downregulated). Error bar associated to each point in the scatter plot represents the standard deviation of the mean of 9 replicated measurements. Metabolites are identified using only the first 30 chars of their full name in Table 2; thus, metabolite indicated by label "28>(31)-3-Aminopiperidine-2,6-dio" corresponds in the scatter plots to points with abscissa 28 and to the entry "(31)-3-Aminopiperidine-2,6-dione, 2TMS" in Table 2.

since the blue polyline connecting points representing metabolites levels in the first of the two compared classes lies almost everywhere above the red polyline representing metabolites levels in the second class. On the contrary, in Fig. 6B the levels of all identified metabolites appear to be very similar in the two compared classes since the green polyline representing metabolites average abundances in class 2Ca-Treatment250 hides almost everywhere the blue line of the class 2Ca-Treatment125.

In order to support the above visual inferences and to make

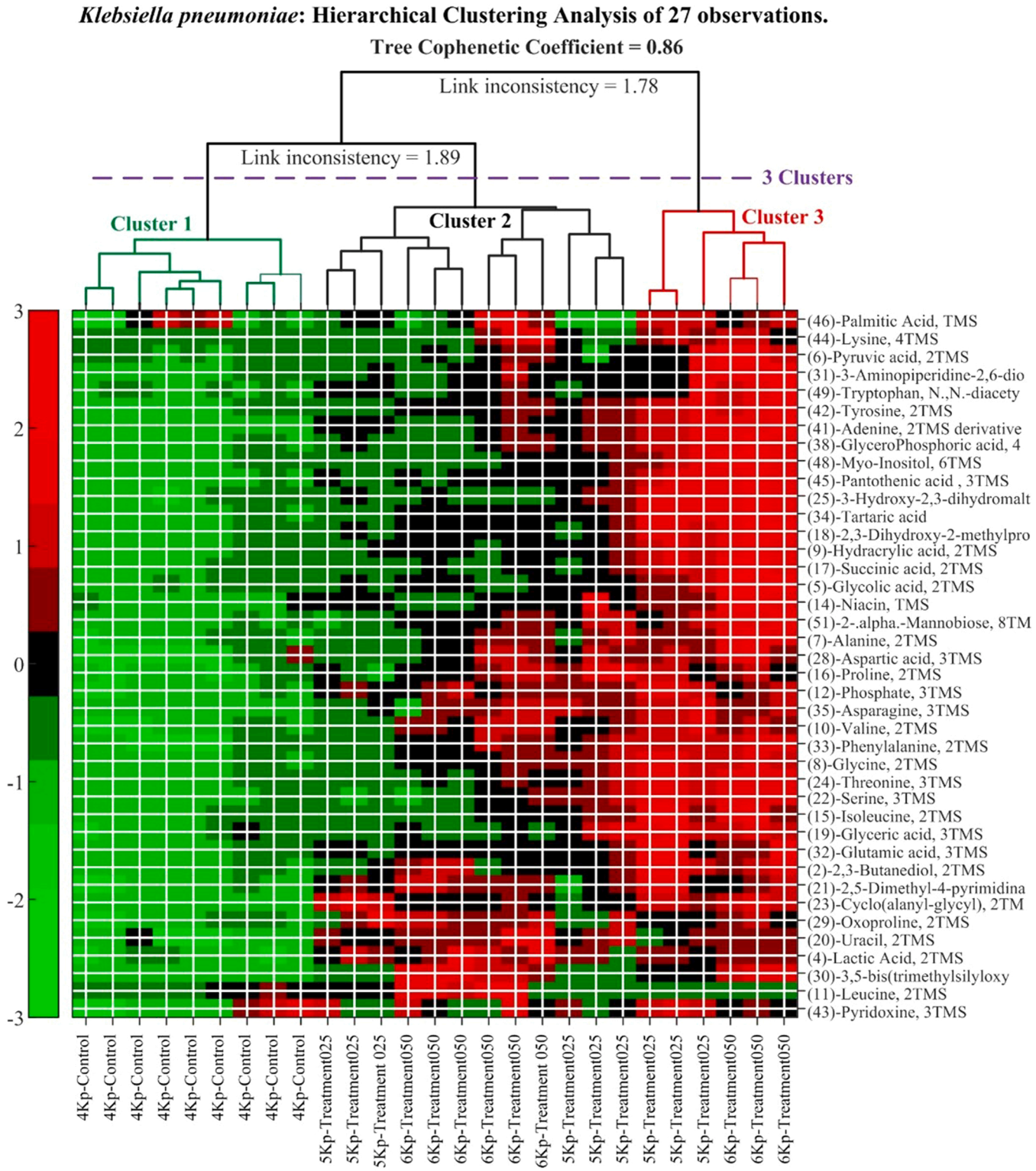

Fig. 7. Clustergram describing Hierarchical Clustering Analysis (HCA) results obtained from metabolomic profiles of biofilm cultures of *K. pneumoniae* grown in presence (i.e., 5Kp-Treatment025 and 6Kp-Treatment050) and absence (i.e., 1Ca-Control) of diplopyrone C. Since rows of the heatmap are standardized to have zero mean and standard deviation 1 (Z-Score standardization), the red colour (positive) of the tile indicates that the metabolite z-score is above the mean and the green colour (negative) indicates that the metabolite z-score is below the mean; obviously, by definition, the mean z-score is zero and corresponds to black colour in the heatmap. Hierarchical Clustering Analysis was performed by setting the distance metric to "Euclidean" and the linkage parameter to "Complete".

comparisons statistically rigorous, in Fig. 6 we report for each metabolite a *p*-value derived by subjecting the averages abundances of each metabolite in the two compared classes to the Student's *t*-test for equal means. At the significance threshold of 0.05, the levels of a given metabolite in the two compared classes may be considered significantly different if the associated *p*-value is lower than 0.05. Thus, we see from Fig. 6A that all metabolites (except, (1)-Propylene glycole and (34)-Arabitol) have *p*-value below the significance threshold. On the contrary, in Fig. 6B, most metabolites have *p*-value above the significance threshold and thus are not significantly different in the two compared classes.

The Fold Change (FC) is the ratio between the two average abundances associated to each metabolite within a pairwise class comparison. According to a principle of caution, in Fig. 6, we consider different two average abundance values if the associated *p*-value is lower than 0.05 and the fold change is higher than 2 or lower than 0.5. Metabolites verifying these conditions are marked in Fig. 7 by labels Up (Upregulated) or Down (Downregulated) while the presence of double equal symbol (i.e., = =) means that the two average values cannot be considered significantly different (either because the *p*-value is higher than the significance threshold or because the fold change is within the range from 0.5 to 2).

Finally, as can easily be seen from Fig. 6A, of the 48 metabolites identified in *C. albicans* cultures 38 are upregulated in class 2Ca-Treatment125 with respect to the untreated 1Ca-Control class. On the contrary, from Fig. 6B, we see that almost all metabolites are marked with the double equal symbol which implies that the metabolite levels are not significantly different in cultures from classes 2Ca-Treatment125 and 3Ca-Treatment250.

3.3.3. *Metabolomics analysis of K. pneumoniae biofilm cultures in presence and absence of diplopyrone C*

Technically, the analysis of data in the IS matrix associated to *K. pneumoniae* moves along lines strictly parallel to the analysis of data in the IS matrix associated to *C. albicans* described in the previous subsection.

Accordingly, when the normalized and standardized IS matrix describing metabolite levels in classes 4Kp-Control, 5Kp-Treatment025 and 6Kp-Treatment050 is presented to the MATLAB's "clustergram" function, results in Fig. 7 are readily obtained. Results in Fig. 7 are extended in Figs S6 and S7.

In the dendrogram in Fig. 7 and Fig. S6, the most inconsistent link lies at a height of about 12 and by cutting the hierarchical tree just below this link (as shown in Fig. 7) three clusters are created. Cluster 1 collects the 9 observations in the untreated 4Kp-Control class, but Cluster 2 and Cluster 3 do not correspond to observations in the nominal classes 5Kp-Treatment025 and 6Kp-Treatment050. The validity of the hierarchical tree in Fig. 7 and Fig. S6 is confirmed by the high value of the tree *cophenetic correlation coefficient* (0.86 out of a maximum of 1) and by the high silhouette value associated to each observation in the Silhouette Plot in Fig. S7.

First, there can be no doubt from Fig. 7 that observations in the untreated 4Kp-Control class, belonging to Cluster 1, are substantially dissimilar from all other observations because they appear to have lower levels of practically all identified metabolites. In fact, observations in Cluster 1 correspond to the nearly uniformly green slice in the heatmap of Fig. 7. This is quite similar to what has been observed for *C. albicans*.

From Fig. 7 and Fig. S6, we see that both Cluster 2 and Cluster 3 collect observations in classes 5Kp-Treatment025 and 6Kp-Treatment050. Because of this, dissimilarity between observations in Cluster 2 and Cluster 3 cannot be ascribed to the change of concentration of diplopyrone C in different observations.

Furthermore, the six observations in Cluster 3 have been acquired by replicated GC-MS analysis of a single biological sample from class 5Kp-Treatment025 and of a single biological sample from class 6Kp-Treatment050. By consequence, what we see in Fig. 7 and Fig. S6 is that one (out of three biological samples in class 5Kp-Treatment025) and one (out of three biological samples in class 6Kp-Treatment050) were found to be quite similar to each other (despite the different concentration of diplopyrone C) and to expose metabolite levels significantly higher than the other four samples collected in Cluster 2 and which appear to be quite similar to each other (despite the different concentrations of diplopyrone C).

Based on the above considerations, we suggest that dissimilarity between observations in Cluster 2 and in Cluster 3 is merely the manifestation of biological variation in the response of *K. pneumoniae* to diplopyrone C exposure.

Fig. 8, which reports results for univariate analysis of data in the normalized IS matrix associated to *K. pneumoniae*, is strictly similar to Fig. 6 both in its general aspect and significance. That is, from Fig. 8A we easily see that of the 40 identified metabolites detected in *K. pneumoniae* cultures, 34 are upregulated in class 5Kp-Treatment025 with respect to class 4Kp-Control. Furthermore, from Fig. 8B we see that the level of 37 metabolites (out of 40) is not significantly different in cultures from classes 5Kp-Treatment025 and 6Kp-Treatment050. This last fact may appear surprising in view of the fact that the 18 observations in classes 5Kp-Treatment025 and 6Kp-Treatment050 are grouped into two dissimilar clusters by the Hierarchical Clustering Analysis. This apparent contradiction is easily resolved by observing that in Fig. 8B are compared the averages of all nine observations in each of the two compared classes while in clustering analysis each observation is considered by itself. In the end, although in classes 5Kp-Treatment025 and 6Kp-Treatment050 there are a few observations which differ from the others, from an average point of view the metabolite levels in these two classes is quite similar. In fact, this is just what one would expect as an effect of biological variation.

4. Discussion

In this study, after the isolation and identification of diplopyrone C from cultures of *D. corticola*, we have investigated the antimicrobial and antibiofilm activities of this compound towards reference strains of common nosocomial pathogens *C. albicans* and *K. pneumoniae* to help meet the urgent need for new antimicrobial agents.

The results of the antimicrobial assays suggest a promising capacity of diplopyrone C to inhibit the growth of these microorganisms. In particular, our findings showed that diplopyrone C was most potent against *K. pneumoniae* compared with *C. albicans*. In fact, it strongly inhibited the growth of *K. pneumoniae* (MIC of 0.500 g L^{-1}).

It is well known that biofilm formation by *C. albicans* and *K. pneumoniae* is an important virulence factor [3,26]. For this reason, diplopyrone C was tested at a number of sub-MIC concentrations for its potential ability to inhibit biofilm formation after 24 h exposure and our results showed that diplopyrone C is able to reduce the adhesion of *C. albicans* by more than 40% at concentration of 0.250 g L^{-1} (corresponding to 1/8 MIC) and *K. pneumoniae* by more than 50% at concentration of 0.050 g L^{-1} (corresponding to 1/10 MIC) (Fig. 2). In addition, the degradative effect of diplopyrone C on mature biofilms was also evaluated observing that the highest concentrations tested (1 g L^{-1}) are able to eradicate at a rate of ~40 and ~50% *C. albicans* and *K. pneumoniae* biofilms, respectively (Fig. 2). Therefore, the mature biofilms of both microorganisms appear to be more tolerant to diplopyrone C. This deduction is also supported by a well-documented low sensitivity of established biofilms to antimicrobial agents [27].

In this study, a footprint metabolomics approach using GC-MS was employed to investigate changes in microbial metabolism caused by the presence of diplopyrone C.

According to the results of biological assays, the changes in the metabolomic profiles induced by diplopyrone C were tracked by enriching the culture medium with two sub-MIC concentrations of the active substance (i.e., 0.125 and 0.250 g L^{-1} for *C. albicans* and 0.025 and 0.050 g L^{-1} for *K. pneumoniae*). A total of 52 extracellular

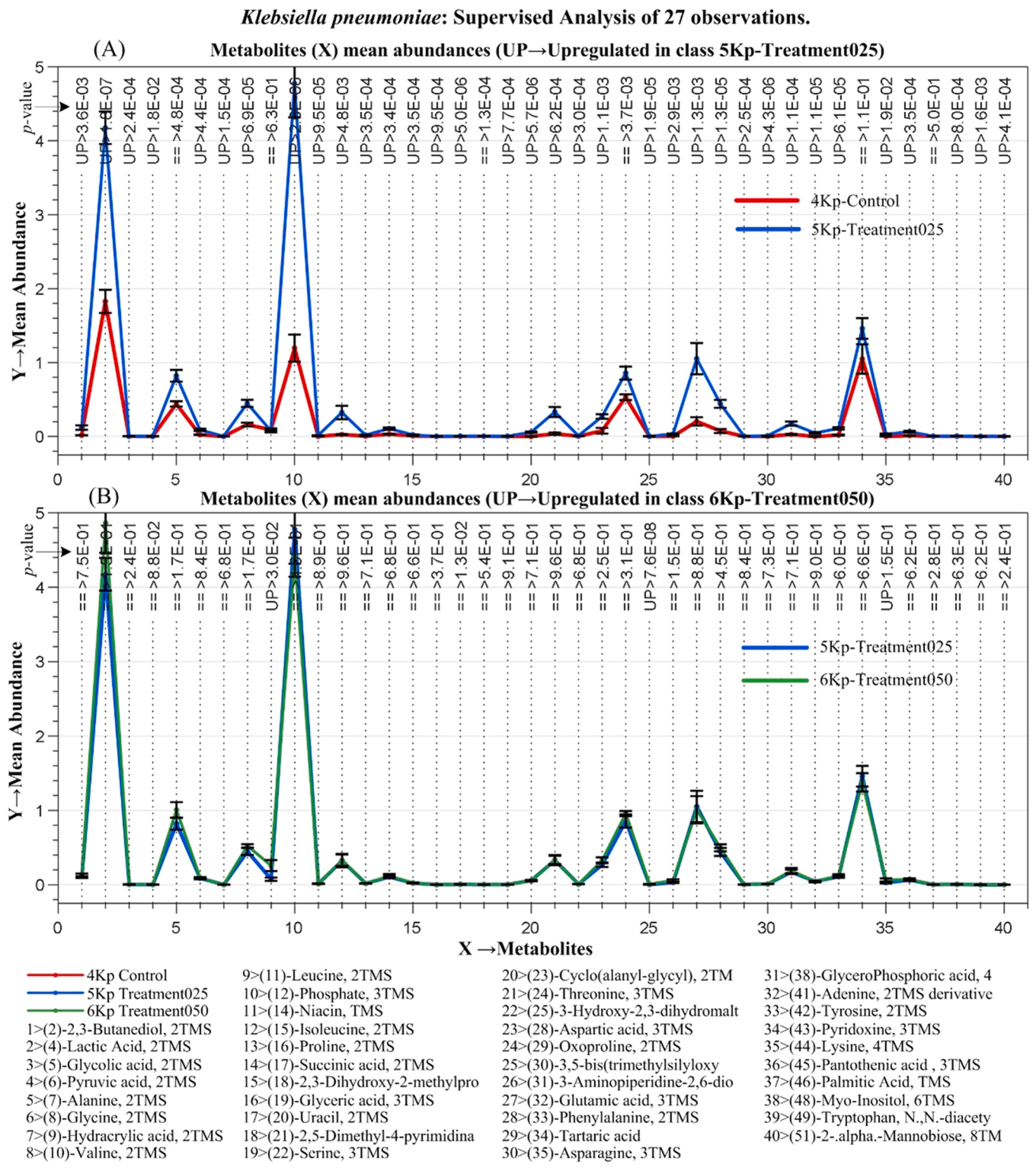

Fig. 8. Results of univariate comparison of biofilm cultures of *K. pneumoniae* in presence (i.e., 0.050 and 0.025 g L^{-1}) and absence of diplopyrone C: (A) 5Kp-Treatment 025 vs. 4Kp-Control; (B) 6Kp-Treatment050 vs. 5Kp-Treatment025. For each metabolite, fold change (FC) is defined as the ratio between mean normalized abundances in the two compared classes. Only metabolites with p-value < 0.05 and fold changes greater than 2 or lower than 0.5 are considered to be differentially expressed in the two compared classes as indicated by labels UP (Upregulated) and DOWN (Downregulated). Error bar associated to each point in the scatter plot represents the standard deviation of the mean of 9 replicated measurements. Metabolites are identified using only the first 30 chars of their full name in Table 2.

metabolites were identified through the six considered biofilm cultures which are related to primary and secondary metabolism (see Fig. 4 and Table 2).

Statistical analysis of the collected GC-MS data (exposed in Figs. 5 and 6 and 7 and 8) shows that metabolic profiles of cultures of *C. albicans* and *K. pneumoniae* treated with diplopyrone C are significantly different from metabolic profiles of control cultures (grown in absence of diplopyrone C).

The culture medium (i.e., tryptic soya broth) employed in this study is a rich medium containing an assortment of compounds available for direct uptake by the microbial cells [28]. In particular, it contains an assortment of amino acids essential for microbial proliferation. Among the metabolic effects induced by diplopyrone C on biofilm cultures, a very evident effect is the reduced uptake of amino acids (e.g., glycine, alanine, glutamic acid, isoleucine, phenylalanine, serine, tyrosine, etc.) from the culture medium (see Figs. 6 and 8). Moreover, the reduced consumption of amino acids in biofilm cultures of *C. albicans* and *K. pneumoniae* was already observed in presence of other antimicrobial agents [28]. A reduced consumption of such important compounds serves as "red flag" on the physiological state of microorganisms. In fact, since amino acids are involved in the tricarboxylic acid (TCA) cycle by being metabolized into intermediates, reduced consumption of these compounds is linked to a decline of TCA cycle activity in biofilm cultures in presence of diplopyrone C. The reduced flow through the TCA cycle automatically switches glycolysis to fermentative pathways to mitigate accumulation of pyruvate (which is the end product of glycolysis) and to increase availability of NAD^+ needed for glycolysis to continue.

Consistent with this interpretation, we observe upregulation of lactate in cultures grown in the presence of diplopyrone C both for *C. albicans* (see Fig. 6A) and *K. pneumoniae* (see Fig. 8A). The upregulation of lactic acid is particularly evident for *K. pneumoniae* cultures as lactic acid is one of the most abundant identified metabolites in bacterial cultures in the presence of diplopyrone C.

In addition to this, *K. pneumoniae* has a range of fermentative pathways that can regenerate NAD^+ from NADH. Most of these fermentative pathways start from pyruvate and produce a number of low molecular weight compounds. In particular, *K. pneumoniae* is in the spotlight for its ability to produce 2,3-butanediol which is a high-value chemical with a wide range of uses in petroleum refining, dyes, adhesives, electronic component cleaning and printing ink industries. In fact, *K. pneumoniae* strains have been metabolically engineered to increase the yield of 2,3-butanediol and allow its production with biological methods which, compared to chemical methods, have low costs, low technical difficulties and significantly reduce environmental pollution [29]. Thus, it is not surprising that we have detected 2,3-butanediol in the *K. pneumoniae* cultures examined in this work (see Table 2), but it may be of interest that the yield of 2,3-butanediol is enhanced by the presence of diplopyrone C in the culture medium. From our data we evaluate a fold change (for 2,3-butanediol) of 7.4 ± 1 by comparing the 9 observations in the untreated *K. pneumoniae* cultures with the 18 observations in cultures treated with 0.025 and 0.050 g L^{-1} of diplopyrone C.

Conversion of pyruvate to 2,3-butanediol takes place according to the half-reaction $2C_3H_3O^- + 4H^+ + 2e^- \rightleftharpoons C_4H_{10}O_2 + 2CO_2$ from which we see that this conversion is a reduction which consumes two electrons so that, for each molecule of 2,3-butanediol produced, one molecule of NAD^+ is regenerated from NADH. Since pyruvate ($C_3H_3O^-$) is a three-carbon molecule and 2,3-butanediol ($C_4H_{10}O_2$) contains four carbon atoms, biosynthesis of 2,3-butanediol from pyruvate requires several enzymatic reactions. First, reaction of two pyruvate molecules, catalysed by acetolactate synthase, yields acetolactate ($C_5H_7O_4^-$) and carbon dioxide. Then, acetolactate is further decarboxylated to acetoin ($C_4H_8O_2$) and the carbonyl function of acetoin is finally reduced to give 2,3-butanediol [29].

1,2-propanediol is, analogously to 2,3-butanediol, another diol with high industrial demand [30]. As can be seen from Fig. 6B, 1,2-propanediol (propylene glycol) is the only metabolite which is upregulated in class 3Ca-Treatment250 with respect to class 2Ca-Treatment125. Closely similar to the production of 1,2-propanediol by *K. pneumoniae*, production of 2,3-butanediol by *C. albicans* in presence of an excess of dyplopirone C stressor provides a way to increase the availability of NAD^+. In fact, an interesting metabolic pathway, based on methylglyoxal, has been proposed for the biosynthesis of 1,2-propanediol in which two NAD^+ molecules are made available for each molecule of 1,2-propanediol produced [30]. Methylglyoxal ($C_3H_4O_2$), released from dihydroxyacetone phosphate ($C_3H_7O_6P$, a glycolysis intermediate) by the action of methylglyoxal synthase, can be converted to 1,2-propanediol ($C_3H_8O_2$) via two alternative routes. In one route, methylglyoxal is first transferred to lactaldehyde ($C_3H_6O_2$) which is then reduced to 1,2-propanediol. Alternatively, methylglyoxal is first transferred to hydroxyacetone ($C_3H_6O_2$) which is then reduced to 1,2-propanediol. In any case, methylglyoxal is converted to 1,2-propanediol by the simple half-reaction $C_3H_4O_2 + 4\,H^+ + 4e^- \rightleftharpoons C_3H_8O_2$ which, unlike the conversion of pyruvate to 2,3-butanediol, consumes four electrons for each molecule of 1,2-propanediol produced [31].

K. pneumoniae also has a metabolic pathway that regenerates NAD^+ from NADH by converting phosphoenolpyruvate (a glycolysis intermediate) into succinate. Thus, in line with the above picture of diplopyrone C-induced metabolic changes, we observed an upregulation of succinate in bacterial cultures treated with diplopyrone C.

On the other hand, biofilm cultures of *C. albicans* show the presence of arabitol and trehalose which are metabolites characteristic of *Candida* species [32].

The level of the polyalcohol arabitol is not significantly affected by the presence of diplopyrone C but the disaccharide trehalose appears to be upregulated in presence of diplopyrone C (see Fig. 6). This result is coherent with the fact that accumulation of trehalose in fungi is associated with periods of reduced growth rate and with the well-known functions of trehalose as cell protector against various stress conditions. In particular, trehalose has attracted considerable attention for its potential in alleviating oxidative stress by acting as ROS (Reactive Oxygen Species) scavenger [33].

Finally, cyclo(alanyl-glycyl) and 3-aminopiperidine-2,6-dione were detected only in treated classes of both microorganisms. These compounds, especially cyclic dipeptides, are product of the secondary metabolism of microorganisms and are often involved in several microbial functions including virulence and pathogenicity [34].

5. Conclusion

The present study demonstrated the antifungal and antibacterial potential of diplopyrone C, a compound recently isolated by us from cultures of the fungus *D. corticola*, against two clinically important pathogens (i.e., the fungus *C. albicans* and the gram-negative bacterium *K. pneumoniae*). According to the MFC/MIC and MBC/MIC ratios, diplopyrone C has fungicidal/bactericidal activity against the two microorganisms tested. Furthermore, this compound is capable of reducing biofilm formation and adhesion and possesses a significant potential for biofilm eradication. Analysis of metabolomic GC-MS data shows a dramatic decrease in nutrients uptake from the culture medium in presence of sub-MIC concentrations of diplopyrone C. In particular, the reduced uptake of amino acids and the simultaneous upregulation of lactate, in diplopyrone C-treated cultures, indicate a decline in TCA cycle activity and a related switch of glycolysis towards lactic acid production. Among other metabolic effects, diplopyrone C enhances the yield of the high-value chemical 2,3-butanediol by *K. pneumoniae*. In conclusion, diplopyrone C can be considered a promising candidate for drug development to meet the urgent need for new antimicrobial agents.

Funding

This research did not receive any specific grant from funding agencies in the public, commercial, or not-for-profit sectors.

CRediT authorship contribution statement

Emilia Galdiero: Writing – review & editing, Supervision, Conceptualization. **Marco Guida:** Supervision, Resources. **Anna Andolfi:** Supervision, Conceptualization. **Angela Maione:** Visualization, Investigation, Formal analysis, Data curation. **Maria Michela Salvatore:** Writing – review & editing, Writing – original draft, Software,

Methodology, Investigation, Formal analysis, Data curation, Conceptualization. **Francesco Salvatore:** Writing – review & editing, Supervision, Software. **Marianna Imparato:** Investigation.

Declaration of Competing Interest

The authors declare that they have no known competing financial interests or personal relationships that could have appeared to influence the work reported in this paper.

Appendix A. Supporting information

Supplementary data associated with this article can be found in the online version at doi:10.1016/j.jpba.2024.116081.

References

[1] A. Talebi Bezmin Abadi, A.A. Rizvanov, T. Haertlé, N.L. Blatt, World Health Organization report: Current crisis of antibiotic resistance, Bionanoscience 9 (2019) 778–788, https://doi.org/10.1007/s12668-019-00658-4 (World).

[2] Z. Zeng, G. Tian, Y. Ding, K. Yang, J. Deng, J. Liu, Epidemiology, antifungal susceptibility, risk factors and mortality of invasive candidiasis in neonates and children in a tertiary teaching hospital in Southwest China, Mycoses 63 (2020) 1164–1174, https://doi.org/10.1111/myc.13146.

[3] J. Kaur, C.J. Nobile, Antifungal drug-resistance mechanisms in *Candida* biofilms, Curr. Opin. Microbiol. 71 (2023) 102237, https://doi.org/10.1016/j.mib.2022.102237.

[4] T. Bardi, V. Pintado, M. Gomez-Rojo, R. Escudero-Sanchez, A. Azzam Lopez, Y. Diez-Remesal, N. Martinez Castro, P. Ruiz-Garbajosa, D. Pestaña, Nosocomial infections associated to COVID-19 in the intensive care unit: clinical characteristics and outcome, Eur. J. Clin. Microbiol. Infect. Dis. 40 (2021) 495–502, https://doi.org/10.1007/s10096-020-04142-w.

[5] N.P. Keller, Fungal secondary metabolism: regulation, function and drug discovery, Nat. Rev. Microbiol. 17 (2019) 167–180, https://doi.org/10.1038/s41579-018-0121-1.

[6] M.M. Salvatore, A. Alves, A. Andolfi, Secondary metabolites of *Lasiodiplodia theobromae*: distribution, chemical diversity, bioactivity, and implications of their occurrence, Toxins 12 (2020) 457, https://doi.org/10.3390/toxins12070457.

[7] M.M. Salvatore, A. Alves, A. Andolfi, Secondary metabolites produced by *Neofusicoccum* species associated with plants: a review, Agriculture 11 (2021) 149, https://doi.org/10.3390/agriculture11020149.

[8] M. Masi, A. Evidente, Sphaeropsidin A: A pimarane diterpene with interesting biological activities and promising practical applications, ChemBioChem 22 (2021) 3263–3269, https://doi.org/10.1002/cbic.202100283.

[9] A. Evidente, A. Andolfi, M. Fiore, E. Spanu, A. Franceschini, L. Maddau, Diplofuranones A and B, two further new 4-monosubstituted 2(3H)-dihydrofuranones produced by *Diplodia corticola*, a fungus pathogen of cork oak, Arkivoc (2007) 318–328, https://doi.org/10.3998/ark.5550190.0008.728.

[10] M.M. Salvatore, I. Di Lelio, M. DellaGreca, R. Nicoletti, F. Salvatore, E. Russo, G. Volpe, A. Becchimanzi, A.E. Mahamedi, A. Berraf-Tebbal, A. Andolfi, Secondary metabolites, including a new 5,6-dihydropyran-2-one, produced by the fungus *Diplodia corticola*. Aphicidal activity of the main metabolite, sphaeropsidin A, Molecules 27 (2022) 2327, https://doi.org/10.3390/molecules27072327.

[11] I.J.S. Fairlamb, L.R. Marrison, J.M. Dickinson, F.J. Lu, J.P. Schmidt, 2-Pyrones possessing antimicrobial and cytotoxic activities, Bioorg. Med. Chem. 12 (2004) 4285–4299, https://doi.org/10.1016/j.bmc.2004.01.051.

[12] F. Sangermano, M. Masi, M. Vivo, P. Ravindra, A. Cimmino, A. Pollice, A. Evidente, V. Calabrò, Higginsianins A and B, two fungal diterpenoid α-pyrones with cytotoxic activity against human cancer cells, Toxicol Vitr. 61 (2019) 104614, https://doi.org/10.1016/j.tiv.2019.104614.

[13] A.R. Gomes, C.L. Varela, E.J. Tavares-da-Silva, F.M.F. Roleira, Epoxide containing molecules: A good or a bad drug design approach, Eur. J. Med. Chem. 201 (2020) 112327, https://doi.org/10.1016/j.ejmech.2020.112327.

[14] A.W. Fothergill, Antifungal Susceptibility Testing: Clinical Laboratory and Standards Institute (CLSI) Methods, : Interact. yeasts, Moulds, Antifung. Agent.: How Detect Resist., Springe (2012) 65–74, https://doi.org/10.1007/978-1-59745-134-5_2.

[15] L.R. Peixoto, P.L. Rosalen, G.L.S. Ferreira, I.A. Freires, F.G. de Carvalho, L. R. Castellano, R.D. de Castro, Antifungal activity, mode of action and anti-biofilm effects of *Laurus nobilis* Linnaeus essential oil against *Candida* spp, Arch. Oral. Biol. 73 (2017) 179–185, https://doi.org/10.1016/j.archoralbio.2016.10.013.

[16] A. Maione, M. Imparato, A. Buonanno, F. Carraturo, A. Schettino, M.T. Schettino, M. Galdiero, E. de Alteriis, M. Guida, E. Galdiero, Anti-biofilm activity of phenyllactic acid against clinical isolates of fluconazole-resistant *Candida albicans*, J. Fungi. 9 (2023) 355, https://doi.org/10.3390/jof9030355.

[17] S. Stepanović, D. Vuković, V. Hola, G. Di Bonaventura, S. Djukić, I. Ćirković, F. Ruzicka, Quantification of biofilm in microtiter plates: Overview of testing conditions and practical recommendations for assessment of biofilm production by staphylococci, Apmis 115 (2007) 891–899, https://doi.org/10.1111/j.1600-0463.2007.apm_630.x.

[18] A. Maione, A. La Pietra, E. de Alteriis, A. Mileo, M. De Falco, M. Guida, E. Galdiero, Effect of myrtenol and its synergistic interactions with antimicrobial drugs in the inhibition of single and mixed biofilms of *Candida auris* and *Klebsiella pneumoniae*, Microorganisms 10 (2022) 1773, https://doi.org/10.3390/microorganisms10091773.

[19] M. Guida, M.M. Salvatore, F. Salvatore, A strategy for GC/MS quantification of polar compounds via their silylated surrogates: silylation and quantification of biological amino acids, J. Anal. Bioanal. Tech. 6 (2015), https://doi.org/10.4172/2155-9872.1000263.

[20] M. Buszewska-Forajta, M. Kordalewska, E. Bartosińska, D. Siluk, R. Kaliszan, Compound identification in metabolomics: a study with the use of two different GC data processing systems, J. Anal. Chem. 71 (2016) 617–623, https://doi.org/10.1134/S1061934816060046.

[21] AMDIS. ⟨www.amdis.net⟩ (accessed October 10, 2023).

[22] MATLAB. ⟨www.mathworks.com⟩ (accessed October 10, 2023).

[23] NIST 20. ⟨https://www.nist.gov/srd/nist-standard-reference-database-1a⟩ (accessed October 10, 2023).

[24] J. Hummel, N. Strehmel, J. Selbig, D. Walther, J. Kopka, Decision tree supported substructure prediction of metabolites from GC-MS profiles, Metabolomics 6 (2010) 322–333, https://doi.org/10.1007/s11306-010-0198-7.

[25] L. Kaufman, P.J. Rousseeuw, Finding Groups in Data: An Introduction to Cluster Analysis, John Wiley & Sons,, Hoboken, NJ, USA, 2009.

[26] C. Vuotto, F. Longo, M.P. Balice, G. Donelli, P.E. Varaldo, Antibiotic resistance related to biofilm formation in *Klebsiella pneumoniae*, Pathogens 3 (2014) 743–758, https://doi.org/10.3390/pathogens3030743.

[27] A. Holmberg, M. Rasmussen, Mature biofilms of Enterococcus faecalis and *Enterococcus faecium* are highly resistant to antibiotics, Diagn. Microbiol. Infect. Dis. 84 (2016) 19–21, https://doi.org/10.1016/j.diagmicrobio.2015.09.012.

[28] E. Galdiero, M.M. Salvatore, A. Maione, F. Carraturo, S. Galdiero, A. Andolfi, F. Salvatore, M. Guida, Impact of the peptide WMR-K on dual-Species biofilm *Candida albicans/Klebsiella pneumoniae* and on the untargeted metabolomic profile, Pathogens 10 (2021) 214, https://doi.org/10.3390/pathogens10020214.

[29] Y. Zhang, D. Liu, Z. Chen, Production of C2-C4 diols from renewable bioresources: New metabolic pathways and metabolic engineering strategies, Biotechnol. Biofuels. 10 (2017) 299, https://doi.org/10.1186/s13068-017-0992-9.

[30] Y. Tao, C. Bu, L. Zou, Y. Hu, Z. Zheng, J. Ouyang, A comprehensive review on microbial production of 1,2-propanediol: micro-organisms, metabolic pathways, and metabolic engineering, Biotechnol. Biofuels. 14 (2021) 216, https://doi.org/10.1186/s13068-021-02067-w.

[31] M.M. Salvatore, F. Salvatore, Strategy to delve into biochemical pathways which include oxidation and reduction based on the concept of total carbon oxidation number of biomolecules, J. Chem. Educ. 100 (2023) 2132–2140, https://doi.org/10.1021/acs.jchemed.1c01282.

[32] E. Galdiero, M.M. Salvatore, A. Maione, E. de Alteriis, A. Andolfi, F. Salvatore, M. Guida, GC-MS-based metabolomics study of single-and dual-species biofilms of *Candida albicans* and *Klebsiella pneumoniae*, Int. J. Mol. Sci. 22 (2021) 3496, https://doi.org/10.3390/ijms22073496.

[33] R. Sánchez-Fresneda, J.P. Guirao-Abad, A. Argüelles, P. González-Párraga, E. Valentín, J.C. Argüelles, Specific stress-induced storage of trehalose, glycerol and d-arabitol in response to oxidative and osmotic stress in *Candida albicans*, Biochem. Biophys. Res. Commun. 430 (2013) 1334–1339, https://doi.org/10.1016/j.bbrc.2012.10.118.

[34] A. Ortiz, E. Sansinenea, Cyclic dipeptides: secondary metabolites isolated from different microorganisms with diverse biological activities, Curr. Med. Chem. 24 (2017) 2773–2780, https://doi.org/10.2174/0929867324666170623092818.